J. Fluid Mech. (1983), *vol.* 131, *pp.* 341–361
Printed in Great Britain

The fluid mechanics of flame tips

By J. BUCKMASTER
University of Illinois, Urbana, Illinois 61801, U.S.A.

AND A. B. CROWLEY
Royal Military College of Science, Shrivenham, Swindon, Wilts, U.K.

(Received 19 January 1982 and in revised form 2 September 1982)

We examine the structure of nominally wedge-shaped or conical premixed flames, of the type that stand at the mouth of a slot or Bunsen burner. A hydrodynamic analysis, justified for slender flames, accounts for the broad features of the flow field, but within a thin zone whose location defines the shape of the flame, heat-conduction, species diffusion and chemical reaction must be accounted for. A simple mathematical description is possible there in the asymptotic limit of infinite activation energy. Near the very extremity of the tip, where the reaction zone is close to the flame axis, this elementary description is no longer valid, and the combustion field is characterized by a free-boundary problem of Stefan type with nonlinear field equations. The numerical treatment of this problem is based on weak solution techniques.

1. Introduction

The inner luminous cone of a Bunsen flame is the result of combustion of the air/fuel mixture that passes up the tube, and this paper is concerned with the nature of the combustion field including details of the gas flow. Such an analysis is justified on several accounts. As one of the oldest known examples of stabilized premixed combustion, Bunsen flames have long been studied in the laboratory; Lewis & von Elbe (1961) summarize many of the conclusions of such investigations. Most importantly, such flames provide one of the simplest examples of a multidimensional combustion field, and thus afford a useful vehicle for escaping from one-dimensional configurations while at the same time avoiding unphysical assumptions or exclusive recourse to numerical computation.

The equations that we shall investigate are

$$\rho(\boldsymbol{q}\cdot\boldsymbol{\nabla})\,Y=\frac{1}{L}\Delta Y-BY\,\mathrm{e}^{-\theta/T}\,H(T-T_{\mathrm{c}}),\tag{1.1a}$$

$$\rho(\boldsymbol{q}\cdot\boldsymbol{\nabla})\,T=\Delta T+BY\,\mathrm{e}^{-\theta/T}\,H(T-T_{\mathrm{c}}),\tag{1.1b}$$

$$B\equiv\frac{Y_{\mathrm{f}}^{2}\theta^{2}}{2(Y_{\mathrm{f}}+T_{\mathrm{f}})^{4}}\exp\frac{\theta}{Y_{\mathrm{f}}+T_{\mathrm{f}}},\tag{1.1c}$$

$$\boldsymbol{\nabla}\cdot(\rho\boldsymbol{q})=0,\quad \rho T=T_{\mathrm{f}},\tag{1.1d,e}$$

$$\rho(\boldsymbol{q}\cdot\boldsymbol{\nabla})\,\boldsymbol{q}=-\boldsymbol{\nabla}p+Pr\left[\Delta\boldsymbol{q}+\tfrac{1}{3}\boldsymbol{\nabla}(\boldsymbol{\nabla}\cdot\boldsymbol{q})\right].\tag{1.1f}$$

Here Y is the mass fraction of the combustible mixture (regarded as a one-component entity), T the temperature, ρ density, $\boldsymbol{q}$ velocity and p pressure. Chemical reaction

is modelled by a one-step irreversible process which is proportional to Y and depends on the temperature through an Arrhenius factor with activation energy θ. H is a Heaviside step function introduced to ensure that there is no reaction in the cold unburnt mixture at the temperature T_f so that T_c is a cut-off temperature where $T_c > T_f$; this is a rational device for resolving the cold-boundary difficulty (Williams 1965). L is the Lewis number, Pr the Prandtl number and B is a parameter whose magnitude is fixed by the precise way in which the equations are non-dimensionalized. Suffice it to say that the choice (1.1*c*) corresponds to an adiabatic flame speed of 1 when $L = 1$, $\theta \to \infty$; for a detailed discussion of the approximations and scalings that lead to the system (1), the reader is referred to Buckmaster & Ludford (1982).

Detailed boundary conditions will be considered in due course, but it may be noted at this time that, roughly speaking, we shall suppose that the unburnt gas lies to the left ($x \to -\infty$), the burnt gas to the right ($x \to +\infty$). Thus in a certain sense we have

$$Y \to Y_f, \quad T \to T_f, \quad \rho \to 1, \quad \boldsymbol{q} \to \boldsymbol{q}_f, \quad p \to p_f = 0 \quad \text{as} \quad x \to -\infty. \tag{1.2}$$

Equations (1.1) have often been simplified by using the constant-density approximation. Then ρ is set equal to 1 and only the equations for T and Y are considered, with $\boldsymbol{q}$ a specified solenoidal velocity field. This severance of the fluid mechanics is a very powerful approximation and makes possible, for example, a complete discussion of the linear stability of the one-dimensional flame or deflagration wave (Sivashinsky 1977). Unrealistic though the approximation might seem, Sivashinsky's results are of great physical interest, providing as they do the first convincing explanation of cellular flames (Markstein 1964). The approximation can be justified if temperature changes throughout the combustion field are small, a necessary condition for which is that the enthalpy liberated by the combustion is small compared to the enthalpy of the cold unburnt mixture, and it has been discussed from that point of view by Matkowsky & Sivashinsky (1979). However, in a typical burner flame the temperature can change from, say, 300 °C on the cold side to 1600 °C on the hot side, and in these circumstances the approximation undoubtedly omits important physics. The goal of the present work is to examine flame tips without adopting the constant-density model, in contrast to previous studies of the problem (Buckmaster 1979; Sivashinsky 1975). It is true that Sivashinsky (1976) formulated the variable-density flame-tip problem in the context of so-called 'slowly varying flames' (SFVs – see Buckmaster & Ludford 1982), but he calculated neither the flow field nor the flame shape when the density is allowed to vary.

A key to the earlier studies of Buckmaster and Sivashinsky, and an essential ingredient of the present one, is the notion that in the limit $\theta \to \infty$ the chemical-reaction term in (1.1.*a*, *b*) can sometimes be replaced by a distribution of Dirac δ-functions. This defines a flame sheet and thus the locus of the flame. There is a continuing tendency in the literature to adopt such a formulation under quite general circumstances, but in fact it can only be justified under certain restrictions. Those adopted here are that L is close to 1 and $T + Y$ is close to $T_f + Y_f$. More precisely, we write

$$L^{-1} = 1 - \theta^{-1}\lambda, \quad \lambda = O(1), \tag{1.3a}$$

$$T + Y = T_f + Y_f + \theta^{-1}\phi + O(\theta^{-2}). \tag{1.3b}$$

ϕ then replaces Y as a dependent variable, and outside of the reaction zone we have

$$\rho(\boldsymbol{q} \cdot \nabla) T = \Delta T, \quad \rho(\boldsymbol{q} \cdot \nabla)\, \phi = \Delta\phi + \lambda \Delta T, \tag{1.4a, b}$$

where T now refers only to the leading term in an asymptotic expansion for the temperature (it seems unnecessarily cumbersome to use the label T_0 for this variable).

The relation (1.3*b*) places restrictions on the allowable boundary conditions. It should also be noted that behind the flame, where no reactants remain (i.e. $Y = 0$), (1.3*b*) implies that the temperature is close to the adiabatic flame temperature $T_f + Y_f$.

Under the restrictions (1.3), replacement of the reaction terms by a distribution of δ-functions can be formally justified, and leads to the jump conditions

$$[\phi] = 0 = [T], \tag{1.5a,b}$$

$$\left[\frac{\partial T}{\partial n}\right] = -\frac{1}{\lambda}\left[\frac{\partial \phi}{\partial n}\right] = -Y_f \exp\frac{\phi}{2(T_f + Y_f)^2} \tag{1.5c,d}$$

$$[\ \ ] \equiv (\ \ )|_{n+0} - (\ \ )|_{n-0}$$

where n is the normal to the reaction surface directed towards the burnt gas. The temperature immediately behind the flame is $T_f + Y_f + \theta^{-1}\phi(n+0)$ and is known as the flame temperature.

Jumps in the other variables and their derivatives can be obtained by further analysis of the flame sheet structure, or by writing the equations in an orthogonal coordinate system locally aligned with the flame sheet and considering the implications for a discontinuity. Thus from Charles' Law,

$$[\rho] = 0, \quad \left[\frac{\partial \rho}{\partial n}\right] = \frac{-T_f}{(T_f + Y_f)^2}\left[\frac{\partial T}{\partial n}\right]. \tag{1.6a,b}$$

From the continuity equation, $$[q_n] = 0. \tag{1.7}$$

From the tangential (s) component of the momentum equation,

$$[q_s] = 0, \quad \left[\frac{\partial q_s}{\partial n}\right] = 0; \tag{1.8a,b}$$

and, from its normal component,

$$[p] = \tfrac{4}{3}Pr\left[\frac{\partial q_n}{\partial n}\right] \tag{1.9}$$

(note that $[\rho q_n^2] = 0$). Finally, using continuity again,

$$\left[\frac{\partial q_n}{\partial n}\right] = \frac{q_n}{T_f + Y_f}\left[\frac{\partial T}{\partial n}\right]. \tag{1.10}$$

Not all of these conditions have to be explicitly invoked in the subsequent analysis.

The hydrodynamic limit

The formulation so far has been on a lengthscale small enough for us to follow the details of the diffusion of heat, mass and vorticity. On a much larger scale these details are lost, and, as is well known, a hydrodynamic description is appropriate. This limit is formally achieved by writing

$$(x, y, z) = D(x', y', z') \tag{1.11}$$

and then letting $D \to \infty$. The effect of this singular limiting process on (1.1*a*, *b*) depends on the relative magnitudes of T and T_c. In any region where $T < T_c$ so that the reaction vanishes identically, the limit equations are

$$(\boldsymbol{q}\cdot\boldsymbol{\nabla}')\,Y = 0 \quad (\boldsymbol{q}\cdot\boldsymbol{\nabla}')\,T = 0, \tag{1.12a,b}$$

where

$$\boldsymbol{\nabla}' \equiv \left(\frac{\partial}{\partial x'}, \frac{\partial}{\partial y'}, \frac{\partial}{\partial z'}\right).$$

It follows that if this region is everywhere penetrated by streamlines from the cold unburnt gas far upstream then $Y = Y_f$ and $T = T_f$ there. On the other hand, if $T > T_c$ the limiting equations are both

$$BY\,\mathrm{e}^{-\theta/T} = 0, \tag{1.13}$$

whence

$$Y \equiv 0. \tag{1.14}$$

In both of these regions the equations of continuity and state are unaltered by the limiting process, but the momentum equation reduces to Euler's form, namely

$$\rho(\boldsymbol{q}\cdot\boldsymbol{\nabla}')\boldsymbol{q} = -\boldsymbol{\nabla}'p. \tag{1.15}$$

Thus the combustion field is divided into two regions, in both of which the governing equations are those of an incompressible inviscid fluid, separated by a discontinuity across which the temperature and density jump by a prescribed amount. Jumps in the other flow variables are constrained by the requirements of mass and momentum conservation. Thus if the subscript '1' refers to the cold scale and '2' to the hot, we have

$$\rho_1 q_{n_1} = \rho_2 q_{n_2}, \quad q_{\perp_1} = q_{\perp_2}, \tag{1.16a,b}$$

$$p_1 + \rho_1 q_{n_1}^2 = p_2 + \rho_2 q_{n_2}^2, \quad Q_f = q_{n_1}. \tag{1.16c,d}$$

Here Q_f is, by definition, the flame speed. This can be calculated by considering the structure of the discontinuity using the full equations (1.1), since in the limit $D \to \infty$ this structure is one-dimensional. Analysis in the limit $\theta \to \infty$, with the restriction (1.3a), leads to the result (Bush & Fendell 1970)

$$Q_f = 1. \tag{1.17}$$

With Q_f specified, the conditions (1.16) uniquely connect the states (1) and (2).

Consider, for example, a simple refraction of a uniform flow (figure 1a). The uniform flow downstream is then defined by

$$\sin\theta = U^{-1}, \quad q_{x_2} = U + Y_f U^{-1} T_f^{-1}, \tag{1.18a,b}$$

$$q_{y_2} = Y_f[1 - U^{-2}]^{\frac{1}{2}} T_f^{-1}, \quad p_2 = -Y_f T_f^{-1}, \quad \rho_2 = T_f(T_f + Y_f)^{-1}. \tag{1.18c,d,e}$$

A flow of this kind is a fundamental feature of burner flames at points sufficiently far from the tip. The essential structure of such flames is sketched in figure 2. The efflux of unburnt gas from the port is essentially a parallel flow with a parabolic distribution in the case of a straight burner, a uniform flow for a nozzle burner. Provided that the port diameter is large compared with the flame thickness, the characteristic feature of the flame on the large scale is the hydrodynamic discontinuity. After refraction by this surface, the streamlines curve until they are once again parallel to the axis. On the smaller scale there is structure near the reaction zone which, at the tip, is quite complicated. Elsewhere this structure is one-dimensional and can be described by seeking a one-dimensional solution of the full equations that depends only on n, the distance normal to the flame sheet. Consider, for example, the structure associated with the refraction of figure 1 (a). Conditions behind the flame sheet are necessarily uniform and so are defined by (1.18) together with

$$T = T_f + Y_f, \quad \phi = 0 \quad (n > 0). \tag{1.19a,b}$$

Ahead of the flame sheet, elementary analysis yields

$$T = T_f + Y_f\,\mathrm{e}^n, \quad \phi = -\lambda n\,\mathrm{e}^n Y_f, \tag{1.20a,b}$$

$$\rho = \frac{T_f}{T_f + Y_f\,\mathrm{e}^n}, \quad p = \frac{Y_f}{T_f}(\tfrac{4}{3}Pr - 1)\,\mathrm{e}^n, \tag{1.20c,d}$$

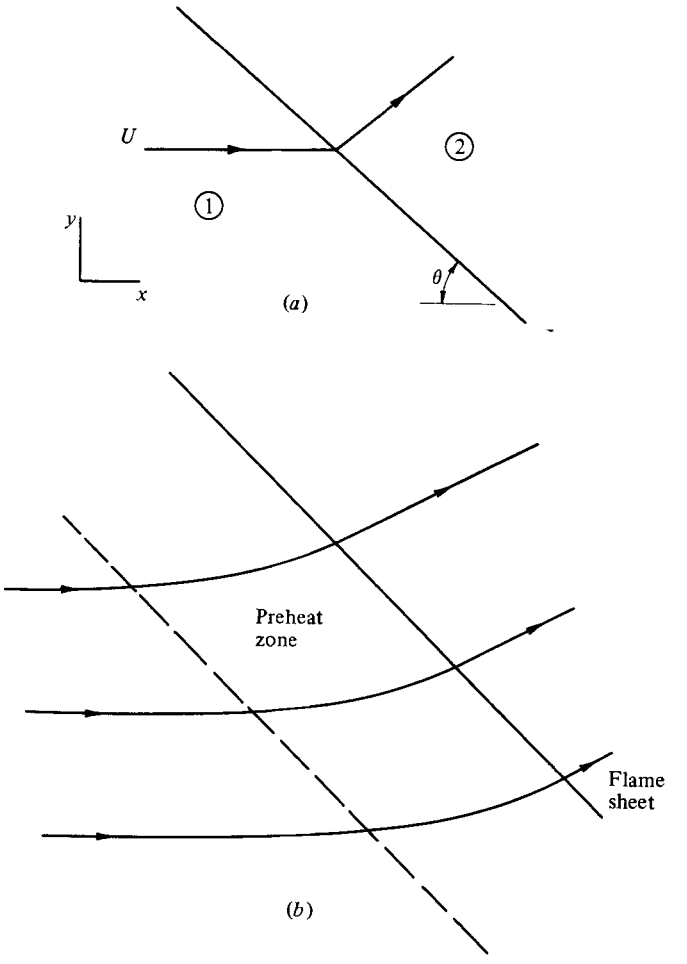

FIGURE 1. (*a*) Simple refraction on the hydrodynamic scale. (*b*) Structure of the refraction.

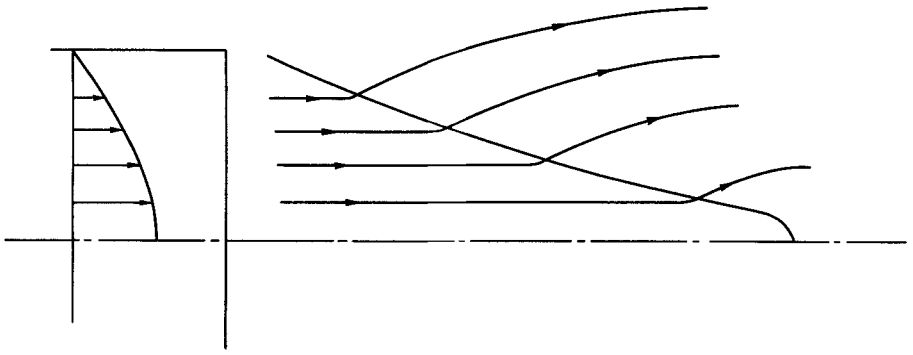

FIGURE 2. Burner flame.

$$q_x = U + \frac{Y_f}{UT_f'} e^n, \quad q_y = \frac{Y_f}{T_f'}(1 - U^{-2})^{\frac{1}{2}} e^n. \tag{1.20e,f}$$

This velocity field is such that q_s is a constant ($= U\cos\theta$) and the normal flux ρq_n is constant ($= U\sin\theta = 1$). Streamlines are sketched in figure 1 (*b*).

2. Slender hydrodynamic flames

2.1. *Plane case*

We now turn to the question of the flow field induced by the presence of a conical or wedge-shaped flame. As already noted, provided that the scale of the flame is large enough and we are not concerned with the details near the reaction zone or tip, a hydrodynamic description will suffice. The complete boundary-value problem, allowing for the presence of the burner and possible nonuniform efflux of gas from the port, is a formidable one. Consequently we shall be content with a description that assumes an unbounded flame which far to the left resembles as closely as possible a uniform cone or wedge, with a uniform flow in the cold gas and simple refraction at the flame front. Moreover we shall assume that the flame is slender (i.e. the wedge or cone angle is small), and then the description can plausibly be expected to be valid near the apex of a real burner flame. The main goals of the analysis are to find the shape of the flame front and to describe the manner in which the refracted streamlines turn back to the original direction far downstream.

The governing equations are

$$\nabla' \cdot \boldsymbol{q} = 0, \quad \rho(\boldsymbol{q} \cdot \nabla')\boldsymbol{q} = -\nabla' p, \tag{2.1a,b}$$

where $\rho = 1$ in the unburnt gas, $T_f/(T_f + Y_f)$ in the burnt gas. If U is a characteristic flow velocity, we shall construct an asymptotic solution valid as $\epsilon \to 0$, where

$$\epsilon = U^{-1}; \tag{2.2}$$

ϵ is a measure of the flame slenderness. No real flame can survive the limit $U \to \infty$, of course, for as U is increased blow-off will eventually occur. But for many burners and mixtures fairly large values of U are possible. Lewis & von Elbe (1971, p. 269), for example, show a plane flame for which $\epsilon \approx 0.1$. For this reason we believe that the limit is worth exploring.

The plane case will be considered in detail, followed by an outline of the corresponding results for the axisymmetric problem.

It is necessary to consider the flows on both the hot and cold sides of the flame, joining them with the jump conditions across the flame front. In this connection it should be noted that for large values of U the formulae (1.18b, c) reduce to

$$q_{x_2} \sim U, \quad q_{y_2} \sim \frac{Y_f}{T_f}. \tag{2.3a,b}$$

That is, the flame front does not affect the x-component of velocity but adds a constant to the y-component.

Consider first the cold side. Defining new variables by

$$\boldsymbol{q} = \left(\frac{1}{\epsilon}u, v\right), \quad p = \frac{1}{\epsilon^2}\overline{p}, \quad (x', y') = \left(\frac{1}{\epsilon}\xi, \eta\right), \tag{2.4a,b,c}$$

the governing equations become

$$\frac{\partial u}{\partial \xi} + \frac{\partial v}{\partial \eta} = 0, \quad \left(u\frac{\partial}{\partial \xi} + v\frac{\partial}{\partial \eta}\right)u = -\frac{\partial \overline{p}}{\partial \xi}, \quad \epsilon^2\left(u\frac{\partial}{\partial \xi} + v\frac{\partial}{\partial \eta}\right)v = -\frac{\partial \overline{p}}{\partial \eta}. \tag{2.5a,b,c}$$

In addition, the condition that the flow upstream of the flame front is irrotational is

$$\frac{\partial u}{\partial \eta} - \epsilon^2\frac{\partial v}{\partial \xi} = 0. \tag{2.6}$$

These equations have general validity for flow inside a slender region.

Consistent with the upstream conditions we further write

$$(u, v) = (1, 0) + \epsilon(u_1, v_1) + \ldots, \tag{2.7a}$$

$$\overline{p} = \epsilon p_1 + \ldots, \tag{2.7b}$$

whence $$u_1 = u_1(\xi), \quad p_1 = -u_1(\xi), \quad v_1 = -u_1'(\xi)\,\eta. \tag{2.8a, b, c}$$

An important feature of this flow is that it is parallel to order $O(\epsilon)$. Then, if the upper surface of the flame front is described by

$$\eta = F(\xi) \sim F_0(\xi), \tag{2.9}$$

the condition that the flame speed equals unity leads to

$$F_0' = -1, \tag{2.10}$$

and to leading order the flame is a uniform wedge:

$$F_0 = -\xi.$$

Consider now the burnt gas. It is appropriate to seek a solution of the form

$$q = \frac{1}{\epsilon}(1, 0) + (\mu_1, \omega_1) + \ldots, \tag{2.11a}$$

$$\overline{p} = \epsilon P_1 + \ldots, \tag{2.11b}$$

with independent variables $$(\xi, \nu) = \epsilon(x', y'), \tag{2.11c}$$

whence $$\frac{\partial \mu_1}{\partial \xi} + \frac{\partial \omega_1}{\partial \nu} = 0, \quad \frac{T_f}{T_f + Y_f}\frac{\partial}{\partial \xi}(\mu_1, \omega_1) = -\left(\frac{\partial}{\partial \xi}, \frac{\partial}{\partial \nu}\right) P_1. \tag{2.12a, b}$$

The jump conditions at the flame front connect this and the solution on the cold side. Indeed,

$$\mu_1 = u_1(\xi), \quad P_1 = -u_1(\xi), \quad \omega_1 = \frac{Y_f}{T_f} \quad (\nu = -\epsilon\xi, \ \xi < 0). \tag{2.13a, b, c}$$

Moreover, symmetry implies that

$$\omega_1 = 0 \quad (\nu = 0, \ \xi > 0). \tag{2.14}$$

Consider the potential solution

$$\mu_{1P} = -\frac{1}{\pi} \ln r \frac{Y_f}{T_f}, \quad \omega_{1P} = \frac{1}{\pi}\phi \frac{Y_f}{T_f}, \tag{2.15a, b}$$

where (r, ϕ) are polar coordinates in the (ξ, ν)-plane. (In this section, which deals exclusively with hydrodynamics, there can be no confusion with the ϕ introduced in (1.3).) This satisfies the condition (2.14), and since at the flame front ϕ is within $O(\epsilon)$ of π it also satisfies (2.13*c*). At the flame front

$$\mu_{1P} = -\frac{1}{\pi} \ln(-\xi) \frac{Y_f}{T_f}, \tag{2.16}$$

so that if $u_1(\xi)$ is given by the same expression this provides a complete solution. However, there is no obvious reason why a shear flow cannot be added to this potential field,

$$\mu_{1r} = f(\nu), \quad \omega_{1r} = 0, \tag{2.17a, b}$$

where $$f(-\epsilon\xi) - \frac{1}{\pi} \ln(-\xi) \frac{Y_f}{T_f} = u_1(\xi). \tag{2.18}$$

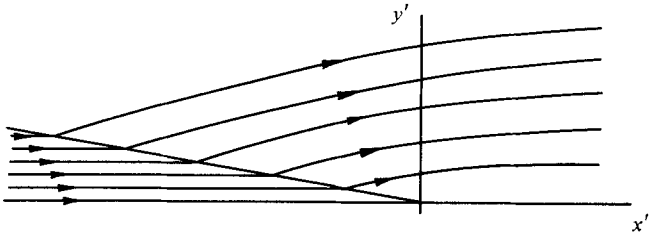

FIGURE 3. Plane hydrodynamic tip drawn for $\epsilon = \tan 10°$, $(\epsilon/\pi)\ Y_f/T_f = 0.1$.

For most choices of u_1 the quantity $\partial\mu_1/\partial\nu$ will be $O(1/\epsilon)$, which is not consistent with the linearization leading to (2.12). However, this difficulty does not arise if u_1 is a multiple of $\ln(-\xi)$. As a special case, if $u_1 = 0$ then

$$f(\nu) = \frac{1}{\pi}\ln\left(\frac{\nu}{\epsilon}\right)\frac{Y_f}{T_f},$$

so that

$$\mu_1 = \mu_{1P} + \mu_{1r} = \frac{Y_f}{\pi T_f}\ln\frac{\sin\phi}{\epsilon}. \tag{2.19}$$

This has an advantage over the potential solution in that it eliminates the singularity in the far field; it has its own pathology, however, namely a wake-like singularity on the positive ξ-axis. There is no immediate way of choosing between (2.15) and (2.19) by local arguments, but fortunately the ambiguity does not affect the value of ω, so that it is possible to draw the streamlines (figure 3).

There is no contradiction between this ambiguity and the well-known relation between flame curvature and generated vorticity (Emmons 1958). Indeed, the vorticity behind the flame is given by the formula (when θ_w is small)

$$\zeta = \frac{Y_f}{T_f}\frac{1}{\theta_w^3}\frac{d\theta_w}{ds},$$

where θ_w is the angle between streamline and flame on the cold side, and s is arclength measured along the flame. Both θ_w and the vorticity considered here are $O(\epsilon)$, corresponding to a (small) flame curvature

$$\frac{d}{d(\epsilon s)}\left(\frac{\theta_w}{\epsilon}\right) = O(\epsilon^2).$$

It should be noted that the curvature of the streamlines downstream of the flame arises as a natural consequence of the flame geometry, and does not require any additional agency such as gravity. In this connection we disagree with the remark of Lewis & von Elbe (1961, p. 271) that 'In a slot burner... [that] ... is upright, the ... streams are forced together again downstream by gravitational buoyancy, and the latter force is chiefly responsible for the curving of the flow lines upward as shown in figure 117*b*...'. The change in kinetic head due to a velocity perturbation q' is comparable to the change in gravitational head over a distance h if $h \sim qq'/g$. Then for the flame considered by Lewis & von Elbe it is easily confirmed that gravity plays a minor role.

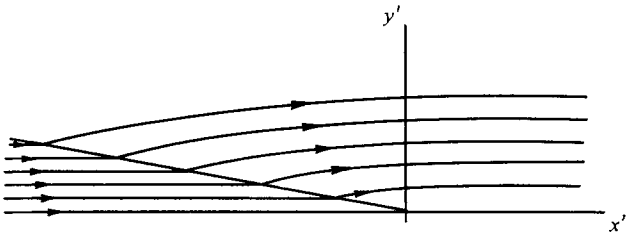

FIGURE 4. Axisymmetric hydrodynamic tip drawn for $\epsilon = \tan 10°$, $(\epsilon/\pi)\, Y_f/T_f = 0.1$.

2.2. *Axisymmetric case*

The discussion for the axisymmetric problem proceeds along very similar lines. On the unburnt side of the flame

$$q_x = \frac{1}{\epsilon}[1 + \epsilon u_1(\xi) + \ldots], \quad q_y = -\frac{1}{2}\epsilon\, u_1'(\xi)\,\eta + \ldots, \tag{2.20a,b}$$

$$\overline{p} = -\epsilon\, u_1(\xi) + \ldots, \quad F_0 = -\xi + \ldots. \tag{2.20c,d}$$

The problem on the burnt side is described by

$$\frac{\partial \mu_1}{\partial \xi} + \frac{1}{\nu}\frac{\partial}{\partial \nu}(\nu\omega_1) = 0, \quad \frac{T_f}{T_f + Y_f}\frac{\partial}{\partial \xi}(\mu_1, \omega_1) = -\left(\frac{\partial}{\partial \xi}, \frac{\partial}{\partial \nu}\right)P, \tag{2.21a,b}$$

$$\omega_1 = \frac{Y_f}{T_f} \quad (\nu = -\epsilon\xi,\ \xi < 0), \tag{2.21c}$$

$$\mu_1 = u_1(\xi), \quad P_1 = -u_1(\xi), \quad \omega_1 = 0 \quad (\nu = 0,\ \xi > 0). \tag{2.21d,e,f}$$

A line of sources whose strength is linear in ξ distributed along the negative ξ-axis defines a potential solution for which μ_1 is $O(1)$, and ω_1 is $O(1)$ near the flame surface, $O(\epsilon)$ elsewhere. This is

$$\mu_1 = 0, \quad \omega_1 = \tfrac{1}{2}\epsilon \tan(\tfrac{1}{2}\phi)\frac{Y_f}{T_f}. \tag{2.22}$$

In contrast with the plane solution, most of the streamline realignment occurs in a small angular neighbourhood of the flame surface (figure 4). A shear flow can be added, just as for the plane case, but the singularities that this introduces make such an addition unattractive.

2.3. *Flame in a non-uniform efflux*

If the efflux from the burner part is not uniform, similar analyses are possible in principle, but the non-trivial shape of the flame front can complicate the exterior problem. However, it is worth noting that this shape can always be calculated without difficulty. Since the interior flow is unaffected to leading order by the presence of the flame, and is, moreover, parallel to order $O(\epsilon)$, the flame-speed condition is

$$1 = -\epsilon\, F_0'(\xi)\, q_x|_{\eta = F_0}. \tag{2.23}$$

Consider, for example, a Poiseuille flow for which

$$q_x = \frac{1}{\epsilon}\left(1 - \frac{\eta^2}{a^2}\right).$$

Integration of (2.23) then yields the shape of a flared cone,

$$\xi = -F_0 + \frac{1}{3}\frac{F_0^3}{a^2}. \tag{2.24}$$

The idea of calculating the flame shape by assuming that the flow is unaffected by the presence of the flame is an old one (Lewis & von Elbe 1961), but can only be justified within the context of slender-flame theory.

3. Structure of the tip

It is not clear that the singular nature of the hydrodynamic solution near the tip can be resolved within the limitations of a hydrodynamic theory. On any lengthscale that is large compared with the preheat-zone thickness, the flame speed is unaffected by the flame configuration and always assumes a value of unity. Thus a smooth tip can only exist if a flame configuration exists for which the interior gas speed near the tip is reduced from $O(\epsilon^{-1})$ values to $O(1)$ values, and, indeed, q_x at the tip itself must equal 1. We shall proceed on the assumption that such a resolution is not possible, or alternatively that it takes place on a length scale that is $o(1)$ (i.e. much smaller than the preheat-zone thickness) so that is superseded by a resolution through the structure equations. It follows that, in examining the tip structure, upstream boundary conditions must be chosen that are compatible with the refraction and associated structure of figure 1, symmetry about the x-axis, and a uniform flow between the refraction and this axis.

The structure equations are simplified by the slender-flame approximation, of course. Define

$$q_x = U\overline{q_x}, \quad x = U\bar{x}, \quad p = U^2\overline{p}, \tag{3.1a,b,c}$$

and consider the limit $U \to \infty$. Then the system (1.1) reduces to

$$\rho(\bar{\boldsymbol{q}}\cdot\bar{\boldsymbol{\nabla}})Y = \frac{1}{L}\nabla_\perp^2 Y - BY\mathrm{e}^{-\theta/T}, \tag{3.2a}$$

$$\rho(\bar{\boldsymbol{q}}\cdot\bar{\boldsymbol{\nabla}})T = \nabla_\perp^2 T + BY\mathrm{e}^{-\theta/T}, \tag{3.2b}$$

$$\bar{\boldsymbol{\nabla}}\cdot(\rho\bar{\boldsymbol{q}}) = 0, \quad \rho T = T_{\mathrm{f}}, \tag{3.2c,d}$$

$$\rho(\bar{\boldsymbol{q}}\cdot\bar{\boldsymbol{\nabla}})\overline{q_x} = -\frac{\partial\overline{p}}{\partial\bar{x}} + Pr\,\nabla_\perp^2\overline{q_x}, \quad 0 = \bar{\boldsymbol{\nabla}}_\perp\overline{p}, \tag{3.2e,f}$$

where

$$\bar{q} = (\overline{q_x}, q_y, q_z), \quad \bar{\boldsymbol{\nabla}} = \left(\frac{\partial}{\partial\bar{x}}, \frac{\partial}{\partial y}, \frac{\partial}{\partial z}\right), \quad \bar{\boldsymbol{\nabla}}_\perp = \left(0, \frac{\partial}{\partial y}, \frac{\partial}{\partial z}\right).$$

There is a corresponding equation for ϕ.

An important advantage of this system is that it is parabolic. In the present context, moreover, the simplification goes much deeper, as we shall see.

The jump conditions at the flame sheet or reaction zone also simplify, chiefly because the normal is orthogonal to the x-axis in the limit. Thus, for plane or axisymmetric tips,

$$-\frac{1}{\lambda}\left[\frac{\partial\phi}{\partial y}\right] = \left[\frac{\partial T}{\partial y}\right] = -Y_{\mathrm{f}}\exp\frac{\phi}{2(Y_{\mathrm{f}}+T_{\mathrm{f}})^2}, \tag{3.3a,b}$$

$$[\overline{p}] = 0, \quad \left[\frac{\partial\overline{q_x}}{\partial y}\right] = 0, \quad \left[\frac{\partial q_y}{\partial y}\right] = \frac{q_n}{T_{\mathrm{f}}+Y_{\mathrm{f}}}\left[\frac{\partial T}{\partial y}\right], \tag{3.3c,d,e}$$

where y is the radial distance in the axisymmetric case. It should be noted that q_n may not be replaced by q_y.

Initial conditions for this parabolic system are defined by (1.19) and (1.20), which are, strictly speaking, only applicable as $\bar{x} \to -\infty$. However, if the flame sheet is located at $y = h_0$ when $\bar{x} = 0$, they may be applied at this finite location provided that h_0 is sufficiently large. Then, replacing n by $y - h_0$ we have

$$\left.\begin{aligned} &\phi = 0, \quad T = T_f + Y_f, && (3.4a, b)\\ &\bar{p} = 0, \quad q_x = 1, \quad q_y = \frac{Y_f}{T_f} && (3.4c, d, e) \end{aligned}\right\} \quad (\bar{x} = 0,\ y > h_0);$$

$$\left.\begin{aligned} &\phi = -\lambda Y_f (y - h_0)\, e^{y-h_0}, \quad T = T_f + Y_f e^{y-h_0}, && (3.5a, b)\\ &\bar{p} = 0, \quad \overline{q_x} = 1, \quad q_y = \frac{Y_f}{T_f} e^{y-h_0} && (3.5c, d, e) \end{aligned}\right\} \quad (\bar{x} = 0, \quad y < h_0).$$

Consistent wth (3.4) and the hydrodynamic analysis, conditions at infinity are

$$\overline{q_x} \to 1, \quad \bar{p} \to 0 \quad \text{as} \quad y \to \infty. \tag{3.6a, b}$$

The momentum equations (3.2e, f) may be eliminated by noting that

$$\overline{q_x} = 1, \quad \bar{p} = 0, \tag{3.7a, b}$$

and then, exterior to the flame sheet,

$$\frac{\partial \rho}{\partial \bar{x}} + \frac{1}{y^\nu}\frac{\partial}{\partial y}(\rho q_y y^\nu) = 0 \quad (\nu = 0, \text{ plane flow};\ \nu = 1, \text{ axisymmetric flow}); \tag{3.8a}$$

$$\rho \frac{\partial T}{\partial \bar{x}} + \rho q_y \frac{\partial T}{\partial y} = \frac{1}{y^\nu}\frac{\partial}{\partial y}\left(y^\nu \frac{\partial T}{\partial y}\right), \tag{3.8b}$$

$$\rho \frac{\partial \phi}{\partial \bar{x}} + \rho q_y \frac{\partial \phi}{\partial y} = \frac{1}{y^\nu}\frac{\partial}{\partial y}\left(y^\nu \frac{\partial \phi}{\partial y}\right) + \frac{\lambda}{y^\nu}\frac{\partial}{\partial y}\left(y^\nu \frac{\partial T}{\partial y}\right). \tag{3.8c}$$

The density may be eliminated from these equations using Charles's Law. Moreover, they imply a simple relation between q_y and the heat flux, so that the number of dependent variables may be reduced to two, namely T and ϕ. Thus writing (3.8b) in conservation form yields

$$\left[y^\nu \frac{\partial}{\partial \bar{x}}(\rho T)\right] - \left[y^\nu T \frac{\partial \rho}{\partial \bar{x}} + T\frac{\partial}{\partial y}(\rho q_y y^\nu)\right] + \frac{\partial}{\partial y}(\rho q_y y^\nu T) = \frac{\partial}{\partial y}\left(y^\nu \frac{\partial T}{\partial y}\right), \tag{3.9}$$

and, since the quantities in square brackets vanish identically, we have

$$q_y = \frac{1}{T_f}\frac{\partial T}{\partial y} + \frac{G(\bar{x})}{y^\nu}, \tag{3.10}$$

where G is an arbitrary function. On the cold side of the flame, the symmetry condition at $y = 0$ implies that G vanishes identically, so that

$$q_y = \frac{1}{T_f}\frac{\partial T}{\partial y}.$$

In particular, at the flame or reaction sheet

$$(q_y)_b = \frac{Y_f}{T_f} \exp \frac{\phi_f}{2(T_f + Y_f)^2}. \tag{3.11}$$

Since q_y is continuous at the flame sheet and $\partial T/\partial y$ vanishes on its hot side, it follows that there

$$q_y = \left[\frac{h(\bar{x})}{y}\right]^{\nu} \frac{Y_f}{T_f} \exp \frac{\phi_f(\bar{x})}{2(T_f+Y_f)^2}, \tag{3.12}$$

where the location of the flame sheet is given by

$$y = h(\bar{x}). \tag{3.13}$$

Using these relations it is only necessary to solve equations for ϕ and T on the cold side of the flame, and an equation for ϕ on the hot side.

3.1. *Flame length*

A complete description of the combustion field is only possible by recourse to the computer, but certain geometrical characteristics of the flame may be deduced analytically. Consider plane flames.

A stream function may be defined by

$$\rho = \rho_b \frac{\partial \psi}{\partial y}, \quad \rho q_y = -\rho_b \frac{\partial \psi}{\partial \bar{x}}, \tag{3.14a,b}$$

with

$$\rho_b \equiv \frac{T_f}{T_f+Y_f},$$

where ψ vanishes at $y = 0$. Thus, on the hot side of the flame,

$$\psi - \psi_b(\bar{x}) = y - h(\bar{x}). \tag{3.15}$$

Here $\psi_b = \psi(\bar{x}, h(\bar{x}))$ is the value of ψ at the flame sheet and

$$\frac{d\psi_b}{d\bar{x}} = -(q_y)_b + h'(\bar{x}),$$

whence

$$\psi_b - \psi_{b0} = h - h_0 - \frac{Y_f}{T_f}\int_0^{\bar{x}} dx \exp \frac{\phi_f(x)}{2(T_f+Y_f)^2}. \tag{3.16}$$

ψ_{b0} is the value of ψ_b at $x = 0$ and may be calculated from the initial conditions (3.5). Thus

$$\psi_{b0} = (T_f+Y_f)\int_0^{h_0} \frac{dy}{T_f+Y_f e^{y-h_0}},$$

which, upon neglecting terms that are $o(1)$ as $h_0 \to \infty$, is

$$\psi_{b0} = \frac{T_f+Y_f}{T_f}\left[h_0 + \ln \frac{T_f}{T_f+Y_f}\right] + o(1). \tag{3.17}$$

Then, from (3.16),

$$\psi_b = \frac{Y_f h_0}{T_f} + \frac{T_f+Y_f}{T_f} \ln \frac{T_f}{T_f+Y_f} + h - \frac{Y_f}{T_f}\int_0^{\bar{x}} dx \exp \frac{\phi_f(x)}{2(T_f+Y_f)^2} + o(1). \tag{3.18}$$

At the tip of the flame where $\bar{x} = \bar{x}_t$, both ψ_b and h vanish, so that

$$h_0 - \bar{x}_t = -\frac{T_f+Y_f}{Y_f} \ln \frac{T_f}{T_f+Y_f} + \int_0^{\bar{x}_t} dx \left[\exp \frac{\phi_f}{2(T_f+Y_f)^2} - 1\right]. \tag{3.19}$$

The right-hand side of the formula represents a 'length deficit' for the flame – it is a measure of the blunting of the uniform wedge because of the structure. In the case

of unit Lewis number ($\lambda = 0$), for which ϕ identically vanishes, this deficit is

$$-\frac{T_f + Y_f}{Y_f} \ln \frac{T_f}{T_f + Y_f}.$$

The deficit is increased (i.e. the flame is blunter) if ϕ_f is positive. This can be understood by recognizing that when ϕ_f is positive the flame temperature exceeds that of the adiabatic flame and there is a corresponding tendency for the flame speed (the component of velocity normal to the flame sheet) to increase.

An analogous treatment is possible for the axisymmetric case, which leads, in the case of $\lambda = 0$, to an expression involving the cross-sectional area of the flame, rather than its length. However, unlike the plane flame, for which deviations from a wedge shape in the far field are exponentially small, for the axisymmetric flame such deviations are algebraic (and non-integrable – see the appendix) and these make an interepretation of the result rather obscure, so that the discussion is omitted.

3.2. *Similarity solution at the tip*

It was noted in an earlier paper (Buckmaster 1979) that, in problems such as the present, a similarity solution valid near the intersection of flame and axis can provide useful local information about the combustion field. Here it is possible to calculate explicitly the local flame curvature. This curvature is responsible for the enhanced flame speed that is necessarily associated with the tip of a closed flame.

In this connection it is appropriate to define new independent variables by

$$\bar{x} - \bar{x}_t = -\rho_b s, \quad \eta = \frac{y}{s^{\frac{1}{2}}}, \tag{3.20a, b}$$

and seek solutions on the hot side of the flame in the form

$$T \sim T_f + Y_f + s^{\frac{1}{2}} f(\eta) + \ldots, \quad \phi \sim \phi_t, \tag{3.21a, b}$$

where the location of the flame sheet is defined by

$$h \sim C s^{\frac{1}{2}}. \tag{3.22}$$

Consider first the axisymmetric problem. The equation for T yields an equation for f, namely

$$f'' + \left(\frac{1}{\eta} - \frac{1}{2}\eta\right) f' + \tfrac{1}{2} f = 0. \tag{3.23}$$

Since f represents the perturbation of the temperature from the value $T_f + Y_f$, this is a linear equation. Symmetry imposes the condition

$$f'(0) = 0, \tag{3.24}$$

and the flame-sheet conditions require

$$f(C) = 0, \quad f'(C) = Y_f \exp \frac{\phi_t}{2(T_f + Y_f)^2}. \tag{3.25a, b}$$

Solutions may be expressed as a contour integral

$$f = \int_{\mathscr{C}} \mathrm{d}t \, \mathrm{e}^{\eta^2 t} \frac{(4t-1)^{\frac{1}{2}}}{t^{\frac{3}{2}}}, \tag{3.26}$$

where $\mathscr{C}$ is any contour in the region of analyticity for which the quantity

$$\mathrm{e}^{\eta^2 t} \frac{(4t-1)^{\frac{3}{2}}}{t^{\frac{1}{2}}}$$

vanishes at both ends. Adopting the principal values for the two multiple-valued functions, one allowable contour encloses the branch cut, and a second emerges from the branch point at $t = \frac{1}{4}$ and passes to infinity along the negative real axis. In this way two independent solutions may be constructed, namely

$$f_1 = \lim_{\epsilon \to 0} \left[\int_{\epsilon}^{\infty} \mathrm{d}t\, \mathrm{e}^{-\eta^2 t} \frac{(\frac{1}{4}+t)^{\frac{1}{2}}}{t^{\frac{3}{2}}} - \frac{1}{\epsilon^{\frac{1}{2}}} \right], \tag{3.27a}$$

$$f_2 = 2 - \int_0^{\frac{1}{4}} \frac{\mathrm{d}t}{t^{\frac{3}{2}}} [\mathrm{e}^{\eta^2 t} (\tfrac{1}{4}-t)^{\frac{1}{2}} - \tfrac{1}{2}]. \tag{3.27b}$$

f_1 is not analytic at $\eta = 0$ and so is not acceptable in the physical problem, and

$$f = c_2 f_2 \tag{3.28}$$

for some constant c_2. Since f_2 is positive at the origin ($f_2(0) = \pi$), but becomes negative for sufficiently large values of η ($f_2 \to -\infty$ as $\eta \to \infty$), there is clearly a value of η for which f vanishes. This defines C (cf. (3.25a)) and therefore the radius $\frac{1}{2}C^2$ of the tip, and numerical computation leads to the estimate $C \approx 2.5$. It is noteworthy that the result is independent of the Lewis number.

In the case of plane tips, the equation for f is

$$f'' - \tfrac{1}{2}\eta f' + \tfrac{1}{2} f = 0. \tag{3.29}$$

One solution is linear and must be discarded because of the condition (3.24). Thus

$$f = c_3 \left[\eta \int_0^{\eta} \frac{\mathrm{d}\eta}{\eta^2} (e^{\frac{1}{4}\eta^2} - 1) - 1 \right] \tag{3.30}$$

for some constant c_3. The quantity in brackets is negative at $\eta = 0$ and approaches positive infinity as $\eta \to \infty$, so that there is a value of η for which f vanishes and this defines $C (\approx 1.85)$.

4. Numerical computations

The numerical method for the computation of the shape of flame tips described by the model equations (3.4), (3.5) and (3.8) is based on the weak-solution approach to moving-boundary problems. In this method the governing equations are cast into conservation form so that the Rankine–Hugoniot conditions at a discontinuity are precisely the jump conditions at the flame front derived earlier (3.3). This being done, the equations may then be solved numerically throughout a fixed region, with the flame front in its interior, without explicitly applying any boundary conditions at the front. This technique has been widely used in moving-boundary problems such as the Stefan problem of heat conduction with change of phase (Kamenomostskaja 1961; Atthey 1974), the solidification of binary alloys (Crowley & Ockendon 1979) and electrochemical machining (Crowley 1979). For further discussion of the application of weak-solution techniques to free and moving boundary problems, the reader is referred to Elliott & Ockendon (1982).

Turning to the model flame-tip equations (3.8), (3.8a, c) may be immediately written in conservative form as

$$\frac{\partial}{\partial \bar{x}} (y^{\nu} \rho) + \frac{\partial}{\partial y} (y^{\nu} \rho q_y) = 0, \tag{4.1}$$

$$\frac{\partial}{\partial \bar{x}} (y^{\nu} \rho \phi) + \frac{\partial}{\partial y} (y^{\nu} \rho q_y \phi) = \frac{\partial}{\partial y} \left(y^{\nu} \frac{\partial \phi}{\partial y} \right) + \lambda \frac{\partial}{\partial y} \left(y^{\nu} \frac{\partial T}{\partial y} \right). \tag{4.2}$$

For (3.8*b*) it is necessary to modify the equation in order that (3.3*b*) may be realized. This may be achieved by writing (3.8*b*) as

$$\frac{\partial}{\partial \bar{x}}(y^\nu \rho T)+\frac{\partial}{\partial y}(y^\nu \rho q_y T)+\frac{\partial}{\partial y}\left\{H(Y_f+T_f-T)\,Y_f\,h^\nu \exp\frac{\phi|_h}{2(T_f+Y_f)^2}\right\}=\frac{\partial}{\partial y}\left(y^\nu \frac{\partial T}{\partial y}\right), \quad (4.3)$$

where the Heaviside function H is defined by

$$H(x)=\begin{cases}0 & (x\leqslant 0),\\ 1 & (x>0).\end{cases}$$

The corresponding jump conditions at the flame front $y=h(\bar{x})$ where $T=T_f+Y_f$ are then

$$[y^\nu \rho]\frac{\mathrm{d}h}{\mathrm{d}\bar{x}}+[y^\nu \rho q_y]=0, \quad (4.4)$$

$$[y^\nu \rho T]\frac{\mathrm{d}h}{\mathrm{d}\bar{x}}+[y^\nu \rho q_y T]+\left[H(T_f+Y_f-T)\,h^\nu Y_f \exp\frac{\phi|_h}{2(T_f+Y_f)^2}\right]=\left[y^\nu \frac{\partial T}{\partial y}\right], \quad (4.5)$$

$$[y^\nu \rho \phi]\frac{\mathrm{d}h}{\mathrm{d}\bar{x}}+[y^\nu \rho q_y \phi]=\left[y^\nu \frac{\partial \phi}{\partial y}\right]+\lambda\left[y^\nu \frac{\partial T}{\partial y}\right]. \quad (4.6)$$

Together with Charles Law, these yield, as required,

$$[\rho]=0=[T]=[\phi], \quad (4.7)$$

$$\frac{1}{\lambda}\left[\frac{\partial \phi}{\partial y}\right]=-\left[\frac{\partial T}{\partial y}\right]=Y_f \exp\frac{\phi|_h}{2(T_f+Y_f)^2}. \quad (4.8)$$

Moreover, direct integration of the temperature equation, using the conditions at $y=0$, gives (cf. (3.10)),

$$q_y=\frac{1}{T_f}\frac{\partial T}{\partial y}+(1-H(T_f+Y_f-T))\frac{Y_f}{T_f}\left(\frac{h}{y}\right)^\nu \exp\frac{\phi|_h}{2(T_f+Y_f)^2}. \quad (4.9)$$

Thus the conservation form of the equations is equivalent to (3.8) together with the jump conditions (3.3), and provides an alternative formulation of the problem.

For numerical solution, the expressions for q_y and T are substituted into the density equation to yield

$$y^\nu \frac{\partial \rho}{\partial \bar{x}}=\frac{\partial}{\partial y}\left(y^\nu \frac{K(\rho)}{\rho}\frac{\partial \rho}{\partial y}\right)-\frac{\partial M}{\partial y}, \quad (4.10)$$

where

$$M(\rho,y)=\frac{Y_f}{T_f}\left\{1-H\left(\rho-\frac{T_f}{T_f+Y_f}\right)\right\}\left(\frac{h}{y}\right)^\nu \exp\frac{\phi|_h}{2(T_f+Y_f)^2}, \quad (4.11)$$

$$K(\rho)=\begin{cases}1 & \left(\rho>\dfrac{T_f}{T_f+Y_f}\right),\\ 0 & \left(\rho\leqslant\dfrac{T_f}{T_f+Y_f}\right).\end{cases} \quad (4.12)$$

The form of $K(\rho)$ on the hot side of the flame is largely arbitrary, since ρ is constant in this region, but it is found that setting $K(\rho)=0$ on the hot side is best computationally, since inevitably $\partial\rho/\partial y$ does not numerically vanish identically. Correspondingly, the ϕ-equation is written

$$\frac{\partial}{\partial \bar{x}}(y^\nu \rho \phi)+\frac{\partial}{\partial y}(y^\nu \rho q_y \phi)=\frac{\partial}{\partial y}\left(y^\nu \frac{\partial \phi}{\partial y}\right)+\lambda\frac{\partial}{\partial y}\left(y^\nu K(\rho)\frac{\partial T}{\partial y}\right).$$

To obtain the results shown in the figures, an explicit finite-difference scheme is used to solve for the density, and an implicit Crank–Nicolson discretization is used for the ϕ-equation. A new value of $\phi|_h$ is than obtained, and iteration is continued on ϕ and q_y until the values are self-consistent. Further discussion of the numerical scheme for this problem may be found in Crowley (1982), and for the related flame-tip problem in which the constant-density approximation is made, that is flame tips without fluid mechanics, in Crowley (1981).

Results

The formulation reveals that $(T-T_f)/Y_f$, $\phi/\lambda Y_f$, ρ, q_y and h depend on only two parameters, namely

$$\Omega = \frac{\lambda Y_f}{(T_f+Y_f)^2}, \quad \frac{T_b}{T_f} = \frac{T_f+Y_f}{T_f}. \tag{4.13}$$

The second of these is the ratio of the burnt-gas temperature to that of the fresh mixture, and is a measure of the importance of variable-density effects. In the limit $T_b/T_f \to 1$, Ω fixed, the problem reduces to the constant-density model treated by Buckmaster (1979). For reasons that are discussed in the appendix, accurate results for axisymmetric tips require a very large initial value for h, so that we have only made calculations for plane tips (solutions for axisymmetric tips for the constant-density model are given by Buckmaster (1979); the identification in that paper of a limiting solution valid as $\Omega \to -\infty$ is incorrect, as the present appendix makes clear). The flame shapes so obtained are drawn in figures 5–7 for different values of Ω and T_b/T_f; these show how the incorporation of variable density has a blunting effect on the tip. Indeed, the theoretical length deficits predicted by (3.19) when $\lambda = 0$ are 1, 1.65 and 2.15 respectively for $T_b/T_f = 1$, 3 or 6, and these compare favourably with the numerical values. Streamline patterns for $\Omega = 0$, $T_b/T_f = 6$ are shown in figure 8.

Whenever the computed flame tip is bulbous in shape there is a possibility of negative flame speeds in which the gas velocity is directed from the burnt side of the flame to the unburnt side. This is not obviously unphysical, since reactants can reach the flame sheet, as required, by diffusion in the y-direction. Nevertheless, in the context of the constant-density model, Buckmaster (1979) proposed to terminate the solution at the point where the flame speed first vanishes, since such solutions correspond to the open tips seen for some mixtures. However, no evidence has since emerged which justifies this choice. In the present situation the gas heating causes the streamlines to diverge, and this is sufficient, for all the solutions shown here, to maintain a positive flame speed everywhere. This will not always be the case. If λ is a large negative quantity and the density ratio across the flame is not too large, negative flame speeds will occur; and a strong temperature dependence of the transport coefficients can lead to negative flame speeds for some of the choices of λ and T_b/T_f considered here.

These results make it clear that the weak-formulation technique is very effective in the treatment of the parabolic free-boundary problem. Unfortunately there is little hope that the technique can be extended to the elliptic problem that arises for modest values of U.

This work was supported by the National Science Foundation, NSF ENG 78-28086, and by the Army Research Office.

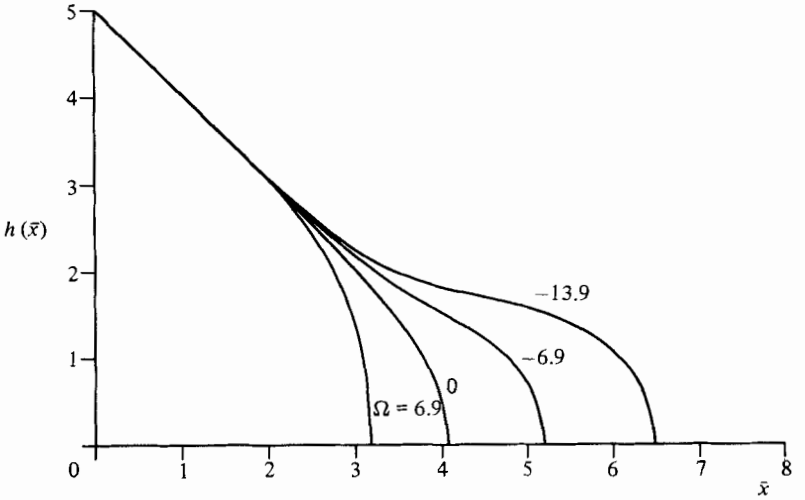

FIGURE 5. Flame-tip shapes for various values of Ω, $T_b/T_f = 1$.

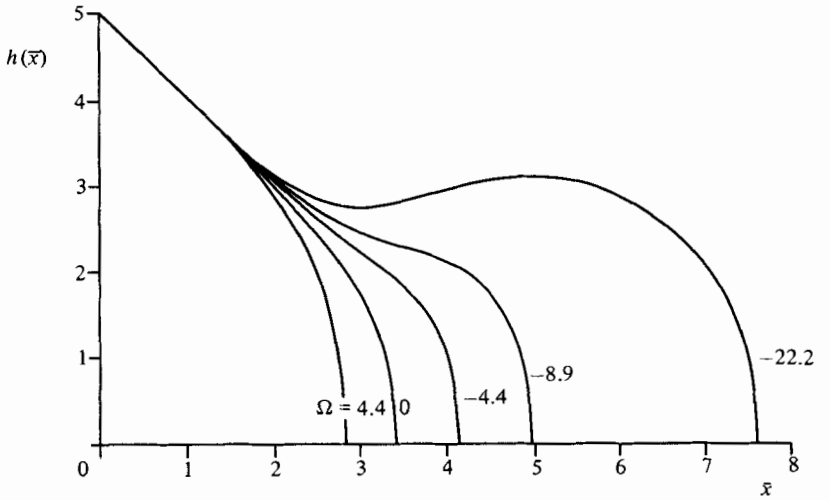

FIGURE 6. Flame-tip shapes for various values of Ω, $T_b/T_f = 3$.

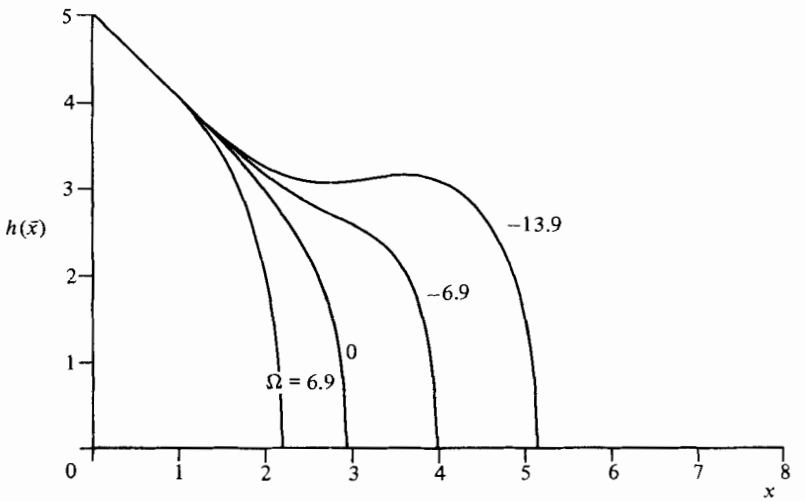

FIGURE 7. Flame-tip shapes for various values of Ω, $T_b/T_f = 6$.

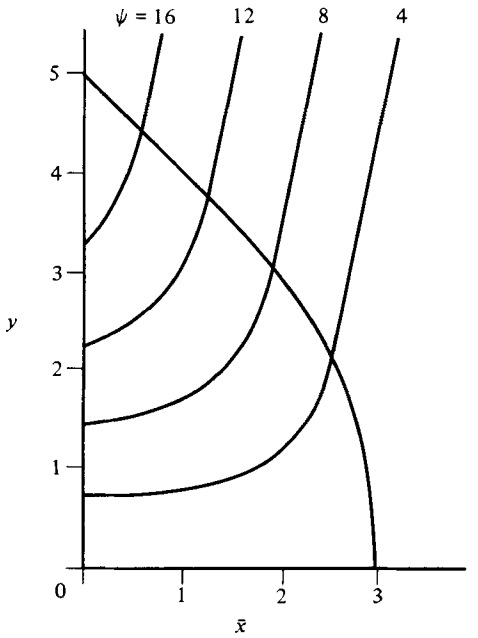

FIGURE 8. Streamlines drawn for $\Omega = 0$, $T_b/T_f = 6$.

Appendix. Far-field description of the axisymmetric tip

In the case of a plane flame approaching a line of symmetry, the presence of the line is first felt when the fringes of the preheat zone intercept it. Since this first tendency of the classical one-dimensional deflagration wave to violate the constraints of the problem is only exponentially small, perturbations in the far field ($x \to -\infty$) have corresponding magnitude. The initial conditions (3.4 and 3.5) are therefore entirely adequate insofar as the numerical computation is concerned, proved that h_0 is moderately large (say 5). For the axisymmetric problem the corresponding perturbations are algebraic, since the one-dimensional structure omits the diffusion term $(1/y)(\partial T/\partial y)$, amongst others. Consequently, although the initial conditions (3.4) and (3.5) are appropriate in principle if h_0 is large enough, in practice they are rather unsatisfactory, and this motivates an examination of the perturbation. The results are of interest in their own right, reflecting as they do the first effects of curvature on the flame in a situation in which the fluid mechanics is realistically accounted for.

Consider first the equation for T, which is

$$\rho \frac{\partial T}{\partial \bar{x}} + \rho q_y \frac{\partial T}{\partial y} = \frac{\partial^2 T}{\partial y^2} + \frac{1}{y}\frac{\partial T}{\partial y}, \tag{A 1}$$

where

$$\rho T = T_f, \quad q_y = \frac{1}{T_f}\frac{\partial T}{\partial y}.$$

We shall assume that, as $\bar{x} \to -\infty$, $\quad \phi_f \sim \dfrac{\beta}{\bar{x}}$

for some β, so that on the cold side of the flame sheet

$$T_b = T_f + Y_f, \quad \left.\frac{\partial T}{\partial y}\right|_b \to Y_f + \frac{\beta Y_f}{2(T_f + Y_f)^2}\frac{1}{\bar{x}} + o\left(\frac{1}{\bar{x}}\right). \tag{A 2a,b}$$

In addition, we shall assume that the position of the flame is defined by

$$\zeta \equiv y+\bar{x}-p(\bar{x}) = 0, \tag{A 3}$$

where

$$p(\bar{x}) = \gamma \ln(-\bar{x})+\ldots. \tag{A 4}$$

It is convenient to use ζ and $\bar{x}$ as independent variables, whence

$$\frac{T_f}{T}\frac{\partial T}{\partial \zeta}+\frac{1}{T}\left(\frac{\partial T}{\partial \zeta}\right)^2 = \frac{\partial^2 T}{\partial \zeta^2}+\frac{1}{\zeta-\bar{x}+p}\frac{\partial T}{\partial \zeta}+\frac{T_f}{T}p'\frac{\partial T}{\partial \zeta}-\frac{T_f}{T}\frac{\partial T}{\partial \bar{x}}. \tag{A 5}$$

Consistent with this,

$$T \sim T_f+Y_f e^{\zeta}+O\left(\frac{1}{\bar{x}}\right),$$

whence, correct to $O(1/\bar{x})$,

$$\frac{T_f}{T^2}\frac{\partial T}{\partial \zeta}+\frac{1}{T^2}\left(\frac{\partial T}{\partial \zeta}\right)^2 = \frac{1}{T}\frac{\partial^2 T}{\partial \zeta^2}-\frac{Y_f e^{\zeta}}{\bar{x}(T_f+Y_f e^{\zeta})}+\frac{p'T e^{\zeta} Y_f}{(T_f+Y_f e^{\zeta})^2}. \tag{A 6}$$

The terms that contain T may be written as exact differentials, whence, integrating once (using $T\rightarrow T_f$ as $\zeta\rightarrow-\infty$),

$$\frac{\partial T}{\partial \zeta}-T = -T_f+\frac{Y_f}{\bar{x}}(T_f+Y_f e^{\zeta})\int_{-\infty}^{\zeta}\frac{ds\, e^s}{T_f+Y_f e^s}-p' Y_f T_f(T_f+Y_f e^{\zeta})\int_{-\infty}^{\zeta}\frac{ds\, e^s}{(T_f+Y_f e^s)^2} \tag{A 7}$$

Integrating once again,

$$T = T_f+Y_f e^{\zeta}-p'\zeta e^{\zeta}Y_f+\frac{e^{\zeta}}{\bar{x}}\int_0^{\zeta} ds\, e^{-s}(T_f+Y_f e^s)\ln\frac{T_f+Y_f e^s}{T_f}+o\left(\frac{1}{\bar{x}}\right), \tag{A 8}$$

which may be represented by

$$T = T_f+Y_f e^{\zeta}+\frac{1}{\bar{x}}f(\zeta)+o\left(\frac{1}{\bar{x}}\right).$$

The heat-flux condition (A 2*b*) at the flame sheet then implies that

$$\frac{\beta Y_f}{2(T_f+Y_f)^2} = (T_f+Y_f)\ln\frac{T_f+Y_f}{T_f}-\bar{x}\,p'(\bar{x})\,Y_f. \tag{A 9}$$

The equation for ϕ is

$$\rho\frac{\partial \phi}{\partial \bar{x}}+\rho q_y\frac{\partial \phi}{\partial y} = \frac{\partial^2 \phi}{\partial y^2}+\frac{1}{y}\frac{\partial \phi}{\partial y}+\lambda\left[\frac{\partial^2 T}{\partial y^2}+\frac{1}{y}\frac{\partial T}{\partial y}\right], \tag{A 10}$$

whence

$$(\rho+\rho q_y)\frac{\partial \phi}{\partial \zeta}-\frac{\partial^2 \phi}{\partial \zeta^2}-\lambda\frac{\partial^2 \phi}{\partial \zeta^2} \approx \rho p'\frac{\partial \phi}{\partial \zeta}-\frac{1}{\bar{x}}\frac{\partial \phi}{\partial \zeta}-\frac{\lambda}{\bar{x}}\frac{\partial T}{\partial \zeta}, \tag{A 11}$$

correct to $O(1/x)$. It follows that on the hot side of the flame

$$\phi \sim \frac{\beta}{\bar{x}}, \tag{A 12}$$

so that the gradient on the cold side is

$$\left.\frac{\partial \phi}{\partial \zeta}\right|_b = -\lambda Y_f-\frac{\lambda\beta Y_f}{2(T+Y_f)^2}\frac{1}{\bar{x}}+o\left(\frac{1}{\bar{x}}\right). \tag{A 13}$$

Noting that

$$\rho+\rho q_y = 1+\frac{1}{\bar{x}}\frac{(f'-f)}{(T_f+Y_f e^{\zeta})}+\ldots, \tag{A 14}$$

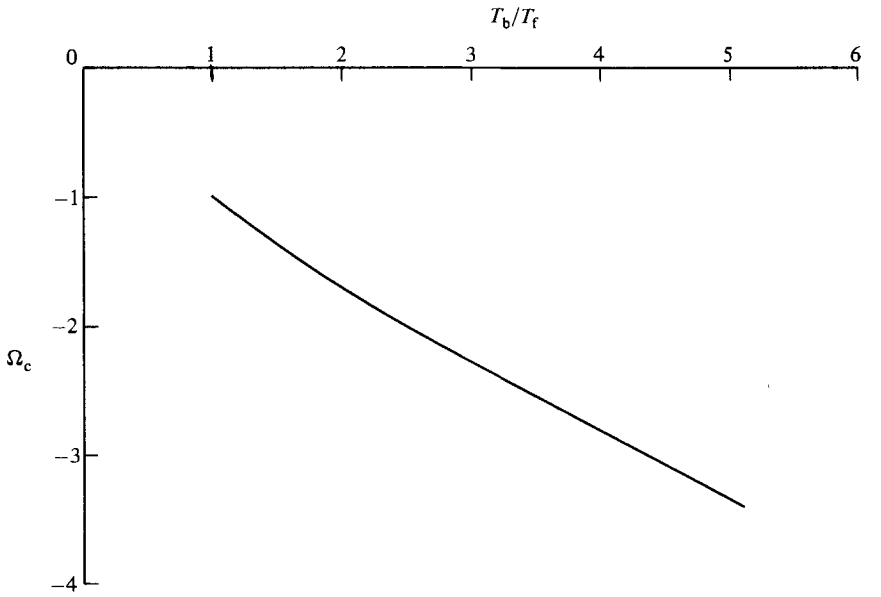

FIGURE 9. Variations of the critical value of Ω with temperature ratio.

we have, on the cold side,

$$\frac{\partial\phi}{\partial\zeta}-\frac{\partial^2\phi}{\partial\zeta^2}-\lambda\frac{\partial^2 T}{\partial\zeta^2}=-\frac{(f'-f)}{\bar{x}(T_f+Y_f e^{\zeta})}\frac{\partial\phi}{\partial\zeta}+\frac{p'T_f}{T_f+Y_f e^{\zeta}}\frac{\partial\phi}{\partial\zeta}-\frac{1}{\bar{x}}\frac{\partial\phi}{\partial\zeta}-\frac{\lambda}{\bar{x}}\frac{\partial T}{\partial\zeta}+\ldots, \quad \text{(A 15)}$$

and since, to leading order,

$$\phi=-\lambda\zeta e^{\zeta}Y_f, \quad \text{(A 16)}$$

the integration of (A 15) implies

$$\phi_b-\frac{\partial\phi}{\partial\xi}\bigg|_b-\lambda\frac{\partial T}{\partial\zeta}\bigg|_b=\frac{\lambda Y_f}{\bar{x}}\int_{-\infty}^{0}ds\frac{f'-f}{T_f+Y_f e^{s}}(s+1)e^{s}-\lambda T_f p'Y_f\int_{-\infty}^{0}ds\frac{(s+1)e^{s}}{T_f+Y_f e^{s}}-\frac{\lambda Y_f}{\bar{x}}, \quad \text{(A 17)}$$

whence

$$\beta=\lambda Y_f\int_{-\infty}^{0}ds\frac{(f'-f)(s+1)e^{s}}{(T_f+Y_f e^{s})}-\lambda T_f\bar{x}p'Y_f\int_{-\infty}^{0}ds\frac{(s+1)e^{s}}{T_f+Y_f e^{s}}-\lambda Y_f. \quad \text{(A 18)}$$

Equations (A 9) and (A 18) together define β and $\bar{x}p'$, whence

$$\beta=\lambda T_f Y_f\int_0^1\frac{dt\ln t}{T_f+Y_f t}. \quad \text{(A 19)}$$

This is positive when λ is negative, so that the flame temperature is less than the adiabatic value (i.e. $\phi_f<0$) when the Lewis number is less than 1 ($\lambda<0$). In addition,

$$p=\ln(-\bar{x})\left\{\frac{T_f+Y_f}{Y_f}\ln\frac{T_f+Y_f}{T_f}-\frac{\lambda T_f Y_f}{2(T_f+Y_f)^2}\int_0^1 dt\frac{\ln t}{T_f+Y_f t}\right\} \quad \text{(A 20)}$$

If λ is greater than some critical value λ_c, this is positive, and in plane section the flame is slightly concave when viewed from the hot side. For $\lambda<\lambda_c$ it is convex. Ω_c is a function of the single parameter T_b/T_f, the density ratio across the flame, and this is plotted in figure 9. As $T_b/T_f\to1$ we have $\lambda_c\to-2T_f^2/Y_f$, the critical Lewis number for a constant-density flame model. This limiting critical value plays a universal role in the behaviour of weakly stretched flames (Buckmaster 1982).

REFERENCES

ATTHEY, D. R. 1974 *J. Inst. Maths Applics* **13**, 353.

BUCKMASTER, J. D. 1979 *Combust. Sci. Tech.* **20**, 33.

BUCKMASTER, J. D. 1982 *Q. J. Mech. Appl. Maths* **35**, 249.

BUCKMASTER, J. D. & LUDFORD, G. S. S. 1982 *Theory of Laminar Flames.* Cambridge University Press.

BUSH, W. & FENDELL, F. 1970 *Combust. Sci. Tech.* **1**, 421.

CROWLEY, A. B. 1979 *J. Inst. Maths Applics* **24**, 43.

CROWLEY, A. B. 1981 In *Proc. Conf. Numerische Behandlung Freier Randwertaufgaben, Oberwolfach, Nov.* 1980. Birkhäuser.

CROWLEY, A. B. 1982 In *Proc. Montecatini Symp. on Free and Moving Boundary Problems.* Pitman.

CROWLEY, A. B. & OCKENDON, J. R. 1979 *Int. J. Heat Mass Transfer* **22**, 941.

ELLIOTT, C. M. & OCKENDON, J. R. 1982 *Weak and Variational Methods for Moving Boundary Problems.* Pitman.

EMMONS, H. 1958 *Fundamentals of Gas Dynamics*, p. 584. Princeton University Press.

KAMENOMOSTASKAJA, S. L. 1961 *Mat. Sb.* **53**, 489.

LEWIS, B. & ELBE, G. VON 1961 *Combustion, Flames and Explosions of Gases.* Academic.

MATOWSKY, B. J. & SIVASHINSKY, G. I. 1979 *SIAM J. Appl. Maths* **37**, 686.

SIVASHINSKY, G. I. 1977 *Combust. Sci. Tech.* **15**, 137.

WILLIAMS, F. 1965 *Combustion Theory*, chap. 5. Addison-Wesley.